

PACS: 61.66.-f

ISSN 1729-4428 (Print)
ISSN 2309-8589 (Online)

O.V. Smitiukh¹, O.M. Yanchuk^{1,2}, O.V. Marchuk¹, Ju.O. Khmaruk¹, M.M. Yatsyshyn³,
O.A. Vyshnevskiy⁴, I.I. Velymchanitsa¹

Electrochemical Synthesis of Nanoparticles of Zinc Oxide Using Film Former MHB 3000 P2

¹Lesya Ukrainka Volyn National University, Lutsk, Ukraine

²Volyn Medical Institute, Lutsk, Ukraine

³Ivan Franko National University of Lviv, Lviv, Ukraine

⁴M.P. Semenenko Institute of Geochemistry, Mineralogy and Ore Formation NAS of Ukraine, Kyiv, Ukraine,

Smitiukh.Oleksandr@vnu.edu.ua

In this work, we present the electrochemical synthesis of zinc oxide in the presence of film former MHB 3000 P2 from a sodium chloride solution and the corresponding concentration of MHB 3000 P2 (in the range of 0.05 to 1.0 g/L). X-ray analysis has been carried out for all 10 samples and synthesized samples are one-phase. A unit cell of the crystalline structure of the nanoparticles is described as the hexagonal crystal system (Space Group $P6_3mc$) and is non-centrosymmetric. The second coordination environment of the crystal system contains three zinc atoms located in tetrahedral positions, which accounts for 3/8 of all tetrahedral voids. While the octahedral voids are empty, allowing for doping with such substances as transition metal atoms that have a tetrahedral environment and are characterized by small atomic radii (e.g., iron, nickel, cobalt). The obtained nanoparticles were also analyzed using SEM. From the obtained images, information regarding the width, length, and thickness of the particles was gathered. It is important to note that the width and length of the particles are quite significant; however, the thickness of the particles ranges from 25 to 27 nm. For the samples synthesized with the lowest surfactant content (from 0 to 0.15 g/L), particles with lengths ranging from 50 to 200 nm predominated quantitatively. Overall, the largest number of particles (by width) is found in the range of 51 to 100 nm for film former concentrations from 0.35 to 0.40 g/L. With an increase in concentration, the number of particles shifts to the range of 50 to 200 nm (by the length). The average thickness and width of the particles do not change significantly with increasing surfactant content, unlike the average length. Overall, it is worth noting the small number of larger particles in each sample; however, these larger particles are crucial for calculating the average sizes.

Keywords: distortion factor; crystalline structure; rare earth metals; elementary cell; tetragonal sulfides.

Received 31 January 2025; Accepted 04 February 2025.

Introduction

Electrochemical synthesis of nanoparticles is an important tool for obtaining modern nanomaterials [1,2].

Zinc oxide (ZnO) nanoparticles with different sizes (20, 44, and 73 nm) have been successfully produced through a hybrid electrochemical-thermal technique. This process utilized an aqueous sodium bicarbonate electrolyte along with sacrificial Zn anodes and cathodes in an undivided cell under galvanostatic conditions at room temperature. The band gaps of the resulting ZnO

nanoparticles were measured at 3.07, 3.12, and 3.13 eV, respectively. The synthesized powder demonstrated remarkable photocatalytic performance, achieving a 92% degradation of methylene blue (MB), suggesting that ZnO nanoparticles can serve as effective semiconductor photocatalysts [3].

Zinc oxide is a highly promising oxide semiconductor material known for its excellent electrical, optical, and piezoelectric properties. It has various applications, including in field-emission displays, solar cells, and gas sensors. Additionally, zinc oxide nanomaterials find use in

electronic, thermal, and quantum devices, as well as in catalysis and wastewater treatment, where they serve as adsorbents and photocatalysts [4-6]

In semiconductor materials science, the size of synthesized nanoparticles and their dispersion is of significant importance. Typically, monodisperse powders are preferred. To this end, various size stabilizers are added to the reaction mixtures. Water-soluble polymers and surfactants are primarily used as stabilizers [7,8]. Therefore, the search for such substances for the synthesis of monodisperse nanometer-sized powders and films is highly relevant.

In the work, we investigate for the first time the effect of the film-forming agent methylhydroxyethylcellulose on the sizes of electrochemically synthesized zinc oxide powders. The product used was branded as MHB 3000 P2. This is methylhydroxyethylcellulose, a non-ionic cellulose ether obtained by adding ethylene oxide to methylcellulose, a white powder that is odorless. It is used as a highly effective water-retaining agent, adhesive, film former, stabilizer, etc. The letter 'B' in the name indicates that more ethylene oxide has been added to achieve a higher level of molecular substitution (MS); DP = 2.3 – the level of powderability (degree of grinding of the product); MS = 1.2 – molecular substitution, in this case, the attachment of an ethylene oxide molecule to a cellobiose molecule at the 5-position of the pyranose ring of cellulose; DS = 4 – degree of substitution of hydroxyl groups; the viscosity of the substance is 4850 mPa•s; NaCl content is 1.14%; the sieving level (in %) on a sieve size of 100 μm÷180 μm is as follows: < 180 micrometer

= 97.40% and <100 micrometer = 63.30%.

I. Experimental details

Nano-sized zinc oxide deposits are obtained by electrolysis of an aqueous solution containing 1M sodium chloride and MHB 3000 P2 with a concentration ranging from 0.05 to 1.0 g/L in galvanostatic mode with two electrodes – a steel cathode with a surface area of 5 cm² and a zinc cylindrical anode at a constant temperature of 90 °C. The method is well-described in the works [8-11]. A magnetic stirrer was used to mix the electrolyte solution. A B5-46 device was used as a DC power supply. For 20 minutes, a constant current of 2.5 A was passed through the electrolyte solution. The numbering of samples, the content of surfactants, and the voltage during electrolysis are presented in Table 1.

II. Results and discussion

X-ray phase analysis has established that all samples are pure zinc oxide in the wurtzite modification. The peaks in all diffractograms completely coincide with the theoretical diffractogram for zinc oxide in the wurtzite modification (SG *P6₃mc.*) (Fig. 1).

The crystalline structure of the synthesized nanooxide can be described as a hexagonal close packing (Fig. 2c), in which zinc atoms are located in the tetrahedral voids. The structure exhibits two types of interatomic distances:

Table 1.

Conditions of electrochemical synthesis involving MHB 3000 P2

Sample №	MD1	MD2	MD3	MD4	MD5	MD6	MD7	MD8	MD9	MD 10
Content of Surfactant, g/L	0.2	0.4	0.6	0.8	1.0	0.05	0.1	0.15	0.25	0.35
Current, V	6.8	6.3	6.9	7.5	7.5	5.3	5.5	5.7	5.7	5.3

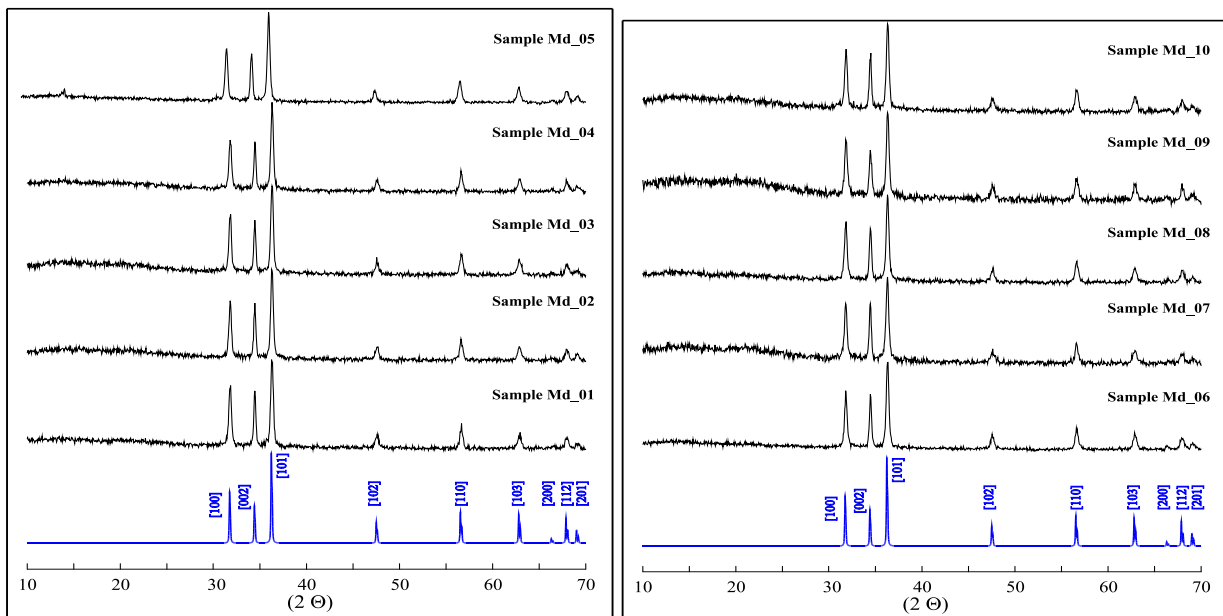


Fig. 1. Diffractograms of bulk deposits obtained for samples Md1-Md10 at a temperature of 90°C, electrolysis time of 20 minutes, current strength of 2.5 A, and different surfactant contents (g/L): Md1-0.20; Md2-0.40; Md3-0.60; Md4-0.80; Md5-1.00; Md6-0.05; Md7-0.10; Md8-0.15; Md9-0.25; Md10-0.30 g/L.

$\delta(\text{Zn-O}) = 1.9598 \text{ \AA}$ and $\delta(\text{Zn-O}) = 2.042 \text{ \AA}$ (Fig. 2a). Overall, the crystalline structure is characterized by a low packing coefficient of the unit cell. This indicates that, based on the second coordination environment (Fig. 2b), we see that 3/8 of the tetrahedral voids are filled with zinc atoms, while all octahedral voids remain unoccupied. Such a material can be doped with various elements, particularly iron or cobalt atoms, which can enhance the magnetic component, among other properties.

Using the Scherrer method, the average thickness of the obtained particles was determined from the maximum peaks of the diffractograms. It turned out that the thickness of the particles calculated by this method [Scherrer's method] [12] is in the range of 25 to 27 nm. The average particle thickness is $26.3 \pm 0.7 \text{ nm}$. The presence of surfactants in the reaction mixture during synthesis practically does not affect the thickness of the synthesized particles. This means that in terms of thickness, the particles are nanosized and uniform.

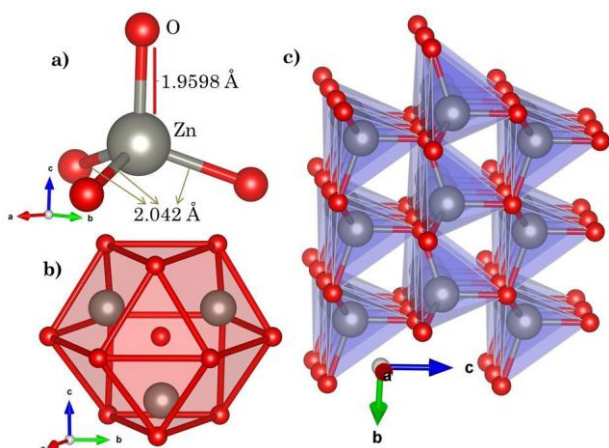


Fig. 2 - Projection of the crystalline structure of synthesized ZnO nanoparticles: a) tetrahedron $[\text{ZnO}_4]^{6-}$; b) second coordination environment; c) arrangement of tetrahedra $[\text{ZnO}_4]^{6-}$.

In addition, the synthesized zinc oxide powders were investigated using scanning electron microscopy (SEM). The obtained photographs for all samples and the sample

synthesized without the participation of surfactants are shown in Fig. 2 and 3.

As seen in Figs 2 and 3, all particles predominantly have paddle-like, flat, occasionally tubular, and occasionally destructured shapes.

To obtain information regarding the average particle sizes and the distribution of the number of particles by size in each photograph, all available particles were numbered and their linear dimensions were determined. The number of particles in each photograph varied. All particles were distributed into 16 ranges: 0–50; 51–100; 101–150; 151–200; 201–250; 251–300; 301–400; 401–500; 501–600; 601–700; 701–800; 801–900; 901–1000; 1001–1250; 1251–1500 nm. Based on the sizes of individual particles, the average length and width of the particles for each synthesized sample were determined. The average sizes of particles synthesized in the presence of surfactants were compared with sample K1, synthesized without surfactants [9], and presented in Table 2.

Table 2.
Dependence of average zinc oxide particle sizes on MHB 3000 P2 content

Content of MHB 3000 P2, g/L	length, nm	width, nm	thickness, nm
0	329	133	25.0
0.05	345	155	26.5
0.10	242	110	27.3
0.15	266	111	25.0
0.20	364	123	25.7
0.25	292	127	25.0
0.35	328	127	26.5
0.40	333	150	27.3
0.60	314	127	27.3
0.80	351	153	26.5
1.00	377	135	25.7

After processing the SEM images, it was found that the length of the particles ranged from 40 to 1300 nm, and the width ranged from 30 to 460 nm.

As seen from Table 2, the average particle sizes in terms of length range from 240 to 380 nm, and in terms of

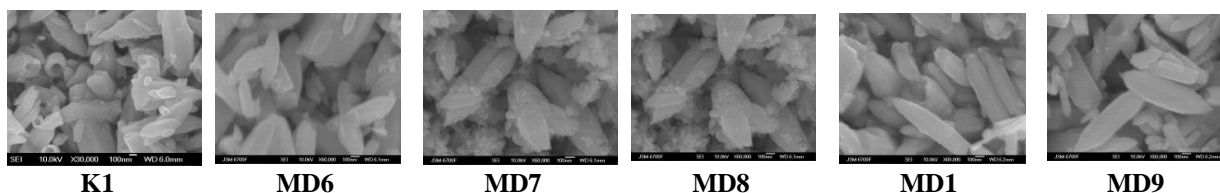


Fig. 2. SEM images of samples synthesized at a current density of 0.5 A/cm² with a MHB 3000 P2 content of 0; 0.05; 0.10; 0.15; 0.20; 0.25 g/L, respectively.



Fig. 3. SEM images of samples synthesized at a current density of 0.5 A/cm² with a MHB 3000 P2 content of 0.35; 0.4; 0.6; 0.8; 1.0 g/L, respectively.

width, from 110 to 155 nm. This dependence is more clearly observed in Fig. 4. As indicated in Table 2 and Fig. 4, the addition of surfactants from 0.1 to 0.35 g/L allows for the production of particles that are smaller in average width compared to the sample obtained without the addition of surfactants. Additionally, in the concentration range of 0.1 to 0.15 g/L, smaller average length particles of zinc oxide are obtained than in the case of the sample synthesized without surfactants. At other concentrations, slightly larger particles are synthesized.

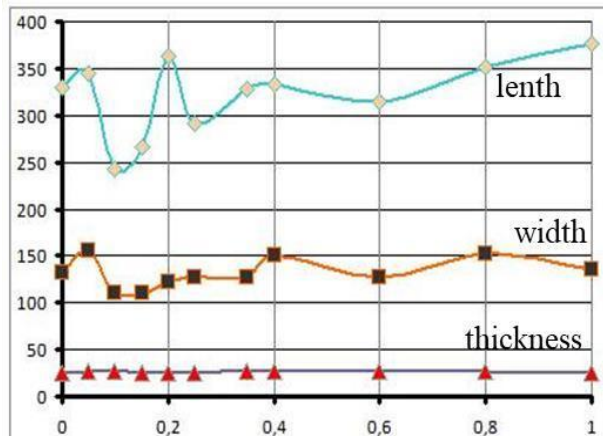


Fig. 4. Dependence of the average linear dimensions of electrochemically synthesized zinc oxide particles on the content of MHB 3000 P2.

It should be noted that a significant variation in particle sizes was observed in each synthesized sample. In particular, the smallest particles measured 40 nm in length, while the largest reached 1.3 μm. The percentages of the number of particles falling into different size ranges were calculated. For the samples synthesized with the lowest surfactant content (from 0 to 0.15 g/L), particles

with lengths ranging from 50 to 200 nm predominated quantitatively; for other samples, a large number of particles were present across a wider range of sizes (see Table 3 and Figure 5). Overall, it is worth noting the small number of larger particles in each sample; however, these larger particles are crucial for calculating the average sizes.

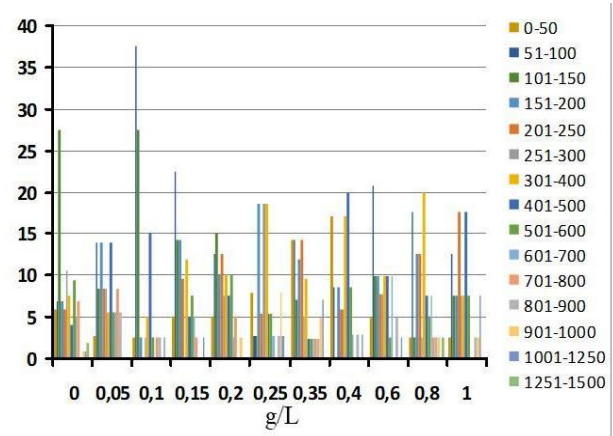


Fig. 5. Histogram of the distribution of the percentage of the number of particles by length depending on the content of MHB 3000 P2.

In Table 4 and Fig. 6 there is a distribution of the percentage of the number of particles by width. As can be seen from Fig. 6 and Table 4, with the exception of samples with a surfactant content of 0.35 and 0.40 g/L, the largest number of particles by width is in the range of 51-100 nm.

Table 3.

Distribution of the percentage of particle number by length by ranges for samples synthesized with MHB 3000 P2

Sample	K1	MD6	MD7	MD8	MD1	MD9	MD10	MD2	MD3	MD4	MD5
Content of Surfactant. g/L	0	0.05	0.1	0.15	0.2	0.25	0.35	0.4	0.6	0.8	1
Range											
0-50	5.9	2.7	2.5	5	5	7.8	14.3	17.1	4.9	2.5	2.5
51-100	6.9	13.9	37.5	22.5	12.5	2.6	14.3	8.6	20.8	17.5	12.5
101-150	27.4	8.3	27.5	14.3	15	2.6	7.1	0	9.8	2.5	7.5
151-200	6.9	13.9	2.5	14.3	10	18.5	11.8	8.6	9.8	12.5	7.5
201-250	5.9	8.3	0	9.5	12.5	5.3	14.3	5.8	7.7	12.5	17.5
251-300	10.6	8.3	2.5	0	7.5	18.5	4.8	5.8	7.7	2.5	7.5
301-400	7.6	5.6	5	11.9	10	18.5	9.5	17.1	9.8	20	7.5
401-500	4	13.9	15	5	7.5	5.3	2.4	20	9.8	7.5	17.5
501-600	9.4	5.6	2.5	7.5	10	5.3	2.4	8.6	2.5	5	7.5
601-700	4.9	5.6	0	5	2.5	2.6	2.4	2.8	9.8	7.5	0
701-800	6.9	8.3	2.5	2.5	5	0	2.4	0	0	2.5	0
801-900	0	5.6	2.5	0	0	2.6	2.4	2.8	4.9	2.5	2.5
901-1000	0.9	0	0	0	2.5	7.8	4.8	0	0	2.5	2.5
1001-1250	0.9	0	2.5	2.5	0	2.6	7.1	2.8	2.5	0	7.5
1251-1500	1.8	0	0	0	0	0	0	0	0	2.5	0

Table 4.

Distribution of the percentage of particle number by width by ranges for samples synthesized with MHB 3000 P2

Sample	K1	MD6	MD7	MD8	MD1	MD9	MD10	MD2	MD3	MD4	MD5
Content of MHB 3000 P2, g/L	0	0.05	0.1	0.15	0.2	0.25	0.35	0.4	0.6	0.8	1
Range											
0-50	14.3	13.9	22.5	11.9	12.5	13	26.2	28.4	24.1	10	15
51-100	42.6	25	37.5	45.2	40	39.5	26.2	5.8	26.8	35	32.5
101-150	14.3	19.4	15	21.4	15	18.5	14.3	20	14.6	12.5	17.5
151-200	9.4	13.9	12.5	9.5	20	15.8	14.3	14.3	14.6	10	12.5
201-250	4	19.4	2.5	9.5	7.5	5.3	4.8	17.1	14.6	12.5	12.5
251-300	6.9	2.8	7.5	2.5	0	5.3	9.4	5.8	4.9	12.5	5
301-400	7.6	0	2.5	0	5	2.6	4.8	8.6	2.5	5	2.5
401-500	0	2.8	0	0	0	0	0	0	0	2.5	2.5
501-600	0.9	2.8	0	0	0	0	0	0	0	0	0

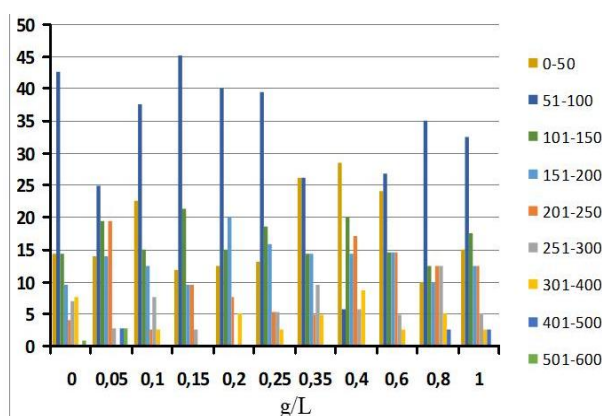


Fig. 6. Histogram of the distribution of the percentage of the number of particles by width depending on the content of MHB 3000 P2.

Conclusions

Increasing the surfactant content does not significantly affect the average particle size. Slightly smaller particles are synthesized at a surfactant content of 0.1 to 0.2 g/l. It is obvious that the studied film former does not contribute to the production of monodisperse powders. However, the large number of particles with cavities indicates that such zinc oxide can be used as a sorbent and catalyst.

Smitiukh Oleksandr – Candidate of Chemical Sciences, Senior Lecturer of the Department of Inorganic and Physical Chemistry; Lesya Ukrainka Volyn National University;

Yanchuk Oleksandr – Candidate of Chemical Sciences, Associate Professor of Volyn Medical Institute;

Marchuk Oleg – Candidate of Chemical Sciences, Associate Professor of the Department of Inorganic and Physical Chemistry, Lesya Ukrainka Volyn National University;

Khmaruk Ju.O. – postgraduate of Lesya Ukrainka Volyn National University;

Yatsyshyn M.M. – Candidate of Chemical Sciences, Associate Professor of the Department of Physical and Colloidal Chemistry, Ivan Franko Lviv National University;

Vyshnevskiy Oleksii A. – Candidate of Chemical Sciences, Associate Professor of M.P. Semenenko Institute of Geochemistry, Mineralogy and Ore Formation NAS of Ukraine;

Velymchanitsa Ivan – student of National Pirogov Memorial Medical University.

- [1] V. Anand, V.C. Srivastava, *Zinc oxide nanoparticles synthesis by electrochemical method: Optimization of parameters for maximization of productivity and characterization*. Journal of Alloys and Compounds, 636, 288 (2015); <https://doi.org/10.1016/j.jallcom.2015.02.189>.
- [2] B. Patella, N. Moukri, G. Regalbuto, C. Cipollina, E. Pace, S.D. Vincenzo, G. Aiello, & R. Inguanta, *Electrochemical Synthesis of Zinc Oxide Nanostructures on Flexible Substrate and Application as an Electrochemical Immunoglobulin-G Immunosensor*. Materials, 15(3), 713 (2022); <https://doi.org/10.3390/ma15030713>.
- [3] K.G. Chandrappa, T.V. Venkatesha, *Electrochemical Synthesis and Photocatalytic Property of Zinc Oxide Nanoparticles*. Nano-Micro Letters, 4(1), 14 (2012); <http://dx.doi.org/10.1007/BF03353686>.

- [4] A. Moezzi, M. Cortie, A. McDonagh, *Aqueous pathways for the formation of zinc oxide nanoparticles*. Dalton Trans, 40, 4871 (2011); <https://doi.org/10.1039/C0DT01748E>.
- [5] S. Bandyopadhyay, *Self-assembled nanoelectronic quantum computer based on the Rashba effect in quantum dots*. Am. Phys. Rev., 61, 13813 (2000); <https://doi.org/10.1103/PhysRevB.61.13813>.
- [6] R. Wahab, I. Hwang, Y. Kim, & H. Shin, *Photocatalytic activity of zinc oxide micro-flowers synthesized via solution method*. Chemical Engineering, Journal, 168 (1), 359 (2011); <https://doi.org/10.1016/j.cej.2011.01.038>.
- [7] S.V. Volkov, Ye.P. Kovalchuk, V.M. Ohenko, O. V. Reshetniak, *Nanokhimiia. Nanosystemy. Nanomaterialy* (K., Naukovadumka, 2008)(In Ukrainian).
- [8] R.V. Korol, O.M. Yanchuk, O.V. Marchuk, et al. *Size Stabilizers in Two-electrode Synthesis of ZnO Nanorods*. Physics and Chemistry of Solid State, 22(2), 380 (2021); <http://dx.doi.org/10.15330/pcss.22.2.380-387>.
- [9] O.V. Smitiukh, O.V. Marchuk., O.M. Yanchuk et al. *Electrochemical Synthesis of Zinc Oxide in the Presence of Surfactant TERGITOL 15-S-5*. Journal of Nano- and Electronic Physics, 16(5), 05032 (2024); [https://doi.org/10.21272/jnep.16\(5\).05032](https://doi.org/10.21272/jnep.16(5).05032).
- [10] O.V. Smitiukh, O.V. Marchuk, O.M. Yanchuk et al. *Electrochemical Synthesis of Zinc Oxide in the Presence of Surfactant FK 06213*. Journal of Nano- and Electronic Physics, 16(6), 06016 (2024); [https://doi.org/10.21272/jnep.16\(6\).06016](https://doi.org/10.21272/jnep.16(6).06016).
- [11] O.V. Smitiukh, O.V. Marchuk, O.M. Yanchuk et al. *Nanoparticles of ZnO/ZnS: Electrochemical Synthesis, Analysis and Prospective*. Journal of Nano- and Electronic Physics, 16(1), 01024 (2024); [https://doi.org/10.21272/jnep.16\(1\).01024](https://doi.org/10.21272/jnep.16(1).01024).
- [12] P. Scherrer, *Bestimmung der Grösse Kolloidteilchen Mittels*. Nachrichten von der Gesellschaft der Wissenschaften, Göttingen, Mathematisch-Physikalische Klasse, 2, 98 (1918).

О.В. Смітюх¹, О.М. Янчук^{1,2}, О.В. Марчук¹, Ю.О. Хмарук¹, М.М. Яцишин³,
О.А. Вишневський⁴, І.І. Велимчаниця¹

Електрохімічний синтез наночастинок цинк оксиду в присутності плівкоутворювача МНВ 3000 Р2

¹Кафедра неорганічної та фізичної хімії, Волинський національний університет імені Лесі Українки, Луцьк, Україна,

²Волинський медичний інститут, Луцьк, Україна

³Львівський національний університет імені Івана Франка, Львів, Україна

⁴Інститут геохімії, мінералогії та рудоутворення ім. М.П. Семененка, Київ, Україна, Smitiukh.Oleksandr@vnu.edu.ua

У цій роботі представлено електрохімічний синтез цинк оксиду у присутності плівкоутворювача МНВ 3000 Р2 з розчину хлориду натрію та відповідної концентрації МНВ 3000 Р2 (в діапазоні від 0,05 до 1,0 г/л). Рентгенографічний аналіз проведено для всіх 10 зразків, синтезовані зразки є однофазними. Елементарна комірка кристалічної структури наночастинок описується як гексагональна кристалічна система (просторова група $R\bar{3}m$) і є нецентросиметричною. Друге координаційне середовище кристалічної системи містить три атоми цинку, що розташовані в тетраедричних позиціях, на які припадає $3/8$ усіх тетраедричних пустот. Наявність октаедричних пустот дозволяє легувати такими речовинами, як атоми перехідних металів, які мають тетраедричне оточення та характеризуються малими атомними радіусами (наприклад, залізо, нікель, кобальт). Отримані наночастинок також аналізували за допомогою СЕМ. З отриманих зображень була зібрана інформація щодо ширини, довжини та товщини частинок. Важливо відзначити, що ширина і довжина частинок досить значні; однак товщина частинок коливається від 25 до 27 нм. Для зразків, синтезованих із найменшим вмістом ПАР (від 0 до 0,15 г/л), кількісно переважали частинки з довжиною від 50 до 200 нм. Загалом, найбільша кількість частинок (за шириною) знаходиться в діапазоні від 51 до 100 нм для концентрацій плівкоутворювача від 0,35 до 0,40 г/л. Зі збільшенням концентрації кількість частинок зміщується в діапазон від 50 до 200 нм (за довжиною). Середня товщина і ширина частинок істотно не змінюються зі збільшенням вмісту ПАР, на відміну від середньої довжини. Загалом, варто відзначити невелике число великих частинок у кожному зразку; однак ці великі частинки є вирішальними для розрахунку середніх розмірів.

Ключові слова: кристалічна структура, наночастинок, розподіл за розмірами, розмірний фактор.